Benefits of continuous source and receiver side wavefields

Stian Hegna (PGS), Tilman Klüver (PGS), and Jostein Lima (PGS)*

Summary

In this paper, we describe a novel acquisition and processing method which makes use of continuous wavefields on both the source and receiver side to extract the response of the earth from marine seismic data. We will describe changes to the typical marine seismic acquisition method and outline the data processing methodology. Special emphasis is given to benefits gained from working with continuous wavefields in terms of improved acquisition efficiency and source side sampling in addition to reduced environmental footprint by lower sound levels.

Introduction

In marine seismic acquisition, several air-guns in arrays are typically triggered simultaneously at pre-defined positions. Then data are recorded for as long as necessary to be able to generate an image of the sub-surface to a desired depth. One seismic shot record is associated with each source array triggering. Each record is assumed to not contain energy from the source excitation associated with the previous record, hence residual energy from previous shots will end up as noise; commonly referred to as shot-generated noise. The air-gun arrays are tuned to emit a wavefield with a wavelet as close as possible to a bandlimited spike. The listening time required to achieve the imaging goals of a survey defines the distance between consecutive shot points. A typical example is 25m shot point interval allowing for 10s listening time at a maximum bottom speed of 2.5m/s (4.86 knots). With typical dual-source acquisition, this results in 50m spacing between shots. This gives significantly coarser sampling than the typical 12.5m channel spacing available on the receiver side.

In recent years, various acquisition and processing methods have been proposed that employ blended or simultaneous source techniques (e.g. Beasley et al., 1998; Berkhout, 2008; Frømyr et al., 2008; Robertsson et al. 2016; Sjøen Pedersen et al., 2016). These methods aim at increasing acquisition efficiency and/or improving spatial sampling of source positions. However, all these methods use the concept of discrete shot records. When the energy from several blended sources is overlapping, 'de-blending' techniques are used to create individual records associated with each of the blended sources. The methods referenced above make use of the same tuned air-gun arrays already described. The wavefields emitted from the blended sources are therefore highly correlated because the wavefield emitted from each source has a wavelet approaching a bandlimited spike.

Methods using encoded source sequences (e.g. Abma and Ross, 2013; Mueller et al., 2014) overcome the similarity between the signals emitted by various sources. The coding in the sequences can be chosen such that the correlation between the signals emitted from multiple sources is reduced. These methods also allow for a reduction of the emitted sound pressure levels as the emitted energy is spread out in time instead of being focused in a short bandlimited spike leading to a reduction in the environmental footprint. These methods all assume discrete shot records.

In this paper, we describe a novel acquisition and processing method that is based on continuous wavefields on both the source and the receiver side. The method allows for a source that is constantly emitting energy while moving. There is no concept of minimum listening time or 'shot' record with specified 'shot point' required. Source energy is spread out in time to reduce the environmental imprint. The movement of all in-sea equipment is taken into account. In the case of towed streamer, the received data are placed into the positions where they were received as if they had been recorded by stationary receivers. If the data is recorded by stationary receivers, this step is not necessary. The emitted source wavefield is deconvolved from the stationary receiver traces to generate receiver gathers containing the response of the earth, i.e. the wavefield being recorded in that receiver position due to point sources emitting a bandlimited spike. The source wavefield emitted by each source can be encoded. This allows for separation of the signal from each individual source in the source deconvolution, enabling simultaneous multiple sources. Data recorded over the length of a sail-line is treated continuously during pre-processing. In the following sections we describe key processing steps and emphasize benefits from working with continuous source and receiver side wavefields in terms of improved source side sampling and reduced environmental imprint.

Methodology

With today's recording systems on seismic vessels data are typically recorded continuously for the length of a sail-line. In the proposed method we correct for sensor responses and apply noise attenuation on the continuous records. After these pre-conditioning steps the receiver motion is corrected for as illustrated in Figure 1. The data is put into stationary receiver traces with a spatial phase shift

$$R_m(t,k) = R(t,k)e^{-ik\Delta x_r(t)}, \quad (1)$$

where R is the recorded data, R_m is the data after motion correction, t and k denote time and horizontal wavenumber

10.1190/segam2018-2995322.1

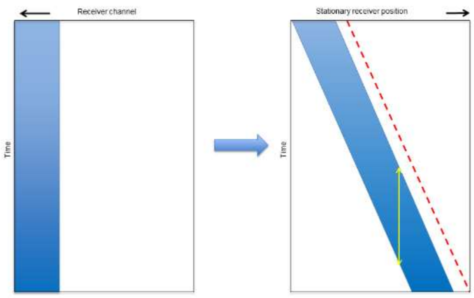

Figure 1: The blue area to the left illustrates a seismic data record recorded continuously, with a temporal extent of a sail line, and a lateral extent corresponding to the streamer length. The blue area to the right represents the seismic data after receiver motion correction. The spatial extent of these data is the length of the sail line plus the streamer length. The red dashed line indicates the position of a source in front of the streamer as a function of time, and the yellow line represents the live data in a stationary receiver position with a temporal length of the streamer length divided by vessel speed.

with respect to the receiver coordinate, respectively, and Δx_r is the receiver motion.

After the receiver motion correction, the recorded pressure and particle motion data are separated into up-going and down-going parts. The methodology is as outlined in Carlson et al. (2007), but applied to the data of one sail-line at once, i.e. to the data as illustrated in the right-hand part of Figure 1, not on a shot record by shot record basis.

In the last step specific to the proposed method, the source wavefield is deconvolved from the stationary receiver trace. We use a multi-dimensional convolutional model to express the data in a stationary receiver trace:

$$R(\omega) = \sum_n E(\omega, k_n) S(\omega, k_n), \qquad (2)$$

where R is the data in the stationary receiver trace, E is the earth response, S is the continuous source wavefield, ω denotes angular frequency, and k is horizontal wavenumber. There is a sum over all source emission angles since all emitted energy is recorded in a single receiver location as illustrated in Figure 2.

The source wavefield contributing to a receiver location including the source ghost can be expressed as follows:

$$S(\omega, k_n) = \sum_t s(t) e^{-i\omega t} e^{-ik_n \Delta x_s(t)} \left(e^{-ik_z z_s(t)} - e^{ik_z z_s(t)}\right), \qquad (3)$$

where $s(t)$ is the signal emitted at time t, $\Delta x_s(t)$ is the lateral position of the source relative to the receiver as a function of time, $z_s(t)$ is the depth of the source as a function of time and k_z is the associated vertical wavenumber.

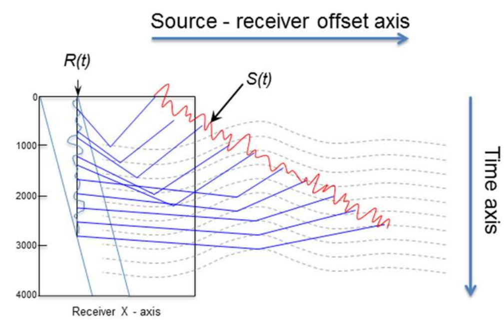

Figure 2: R(t) is a stationary receiver trace as a function of time, and S(t) are the source signals emitted as a function of time in different offsets relative to the receiver location. The grey dashed lines represent one reflector in the sub-surface, and the blue lines represent some of the ray-paths from the source reflected at the sub-surface reflector and received in the stationary receiver position.

In order to deconvolve the source wavefield from the receiver wavefield, an inverse solution to the forward modelling in equation (2) has to be found. We solve this problem iteratively. Since the source emission angle in a single receiver location is unknown, the energy is placed in all possible angles and the source wavefield is deconvolved. This guarantees that the signal associated with the response of the earth is focused in the correct locations. However, noise is generated as well since a lot of energy is placed in incorrect angles. Coherent energy is extracted from the deconvolution result and its contribution to the receiver trace is modelled and subtracted to generate a residual receiver trace containing signals that have not yet been explained. The process starts again with deconvolving the source wavefield from the residual receiver trace. In each iteration the explained signal is accumulated. The amount of noise generated decreases as more and more signal is explained. When no coherent signal can be extracted anymore, the residual deconvolution result is added in order to not lose any signal in the end result.

We illustrate this step using a synthetic data example where we modelled a receiver trace over an earth model containing three reflectors and seven point diffractors using a source continuously emitting band-limited Gaussian white noise while moving. The modelled receiver trace is shown at the top of Figure 3. It has a length of 3200s which corresponds to a streamer length of 8000m and a vessel speed of 2.5m/s. The final deconvolution result is shown at the bottom of Figure 3 together with a modelled reference earth response and the difference between the two. The energy level in the difference is very small illustrating the effectiveness of the iterative source deconvolution method.

A seismic source emitting band-limited white noise does not exist. It is however possible to approach the properties of

10.1190/segam2018-2995322.1

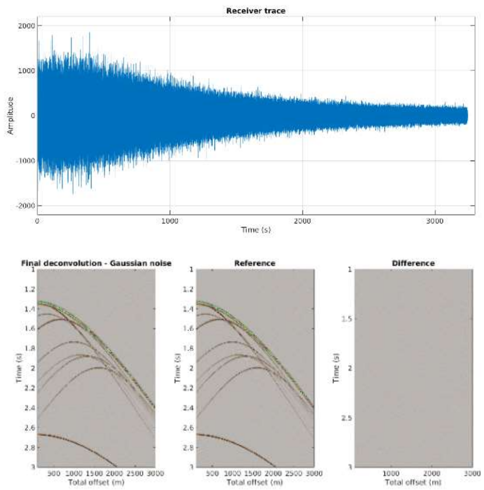

Figure 3: Top: Simulated receiver trace in a stationary position containing more than 3000 seconds of signals received continuously. Bottom: Results from the iterative source deconvolution process shown to the left. The image in the middle shows the desired output, and the image to the right shows the difference between the deconvolution result and the desired result.

white noise by triggering individual air-guns densely with randomized time intervals. Typically, a seismic vessel tows six strings of air-guns allowing for the layout shown in Figure 4. Each string is equipped with three different volumes in a different order. The air-guns are triggered one by one cycling through the strings and the air-guns within a string in a pre-defined order. With a mean trigger time interval in the order of 300ms and a suitable randomization interval, a source wavefield is generated which approaches the properties of white noise.

Since each string is set up differently, the cross-correlation between the wavefields emitted from individual strings is minimized. This allows us to separate the wavefields from all six strings during the source deconvolution resulting in a hexa-source setup. After the deconvolution, individual sources can be combined if desirable. Figure 5 shows the deconvolution result for a receiver trace modelled in the same location over the same geological model as used for Figure 3, but using the setup shown in Figure 4 with a string separation of 200m. The different temporal and spatial position of the diffraction events illustrates the 3D character of the simulation. The residual noise level is only slightly increased compared to the single source case.

Improved source side sampling

At 4ms temporal sampling interval, the offset increment in the output receiver gather from the source deconvolution is 6.25m, i.e. the signal is fully de-aliased. This is facilitated by the continuous source wavefield. With 12.5 m channel

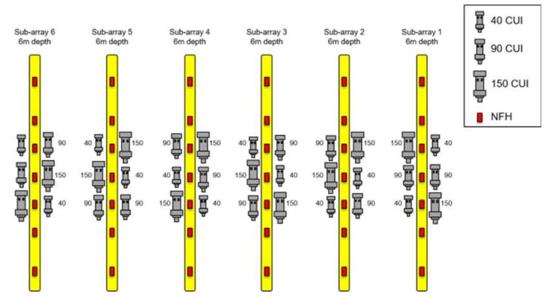

Figure 4: Six strings with 40, 90 and 150 cubic-inch air-guns on each. The configuration of the three volumes is different on each sub-array to provide additional encoding of the wavefield emitted from each string.

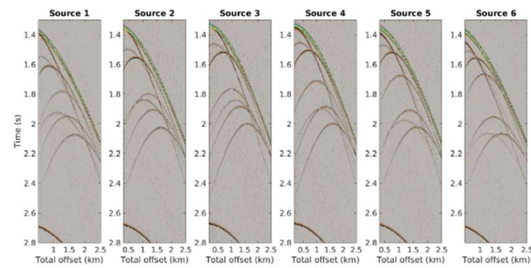

Figure 5: Result of deconvolving the source wavefield into six common receiver gathers with earth responses extracted from one stationary receiver location based on the source configuration shown in Figure 4. The spacing between the strings of air-guns was 200m.

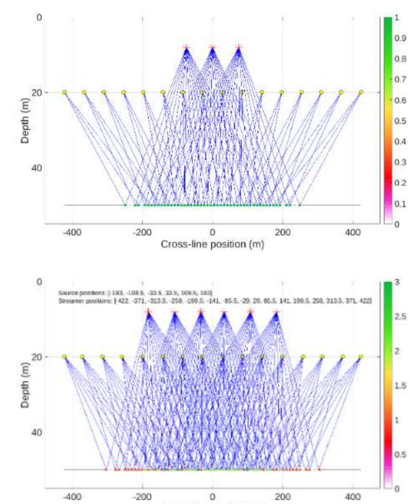

Figure 6: Top: Towed streamer configuration with 3 sources, 75 m separation, and 16 streamers, 56.25 m separation. The nominal sail line spacing with this configuration is 450 m. The colored squares at the reflector level shows the number of hits per bin in the cross-line direction. Bottom: A 6 source, 16 streamer, configuration determined through an optimization process. The nominal sail line separation would is 550 m for this configuration. The source and streamer positions are listed in the upper part of the image.

10.1190/segam2018-2995322.1

spacing on the receiver side, the receiver gathers are anti-alias protected to 12.5m spacing as well to create symmetric wavenumber content on the source and receiver side in the inline direction. A shot point spacing of 12.5 m along the line is otherwise only achievable with very short records or blended acquisition. The proposed method therefore generates higher density band-limited point sources along the line.

When several sources with different coding are emitting energy simultaneously, they can be separated during the iterative source deconvolution as illustrated in Figure 5. This potentially allows great flexibility in survey design. When optimizing source and streamer positions, configurations can be found which optimally combine survey efficiency with sampling requirements. For example, the hexa-source configuration shown in Figure 6 would allow for denser crossline CMP spacing together with increased sail-line distance, i.e. increased efficiency, compared to the triple source configuration shown in the same Figure. At present this is a concept and has not been tested.

Reduced environmental footprint

One of the main benefits of spreading the emitted wavefield from the sources in time is a potential reduction of sound levels. Traditionally, in the order of 30-35 air-guns in a source array are triggered simultaneously. By triggering one air-gun at the time the peak sound pressure levels (peak SPL) are reduced significantly compared to triggering a 4130 cubic-inch source array as illustrated in Figure 7. A comparison between the SEL, integrated over 10 s, of the standard array and the triggering of individual air-guns is shown in Figure 8 for one direction from the source. We can see in that modelling study that the SEL is lower when triggering individual air-guns.

Both the peak SPL and SEL are here determined through modelling assuming wave propagation through a homogeneous medium with properties of water and a sea surface reflection coefficient of -1. This modeling approach is widely used in permitting processes and follows the standard metrics used in the industry today (Goertz et al., 2013). Still, it is important to note that the SEL results presented here should be considered as a relative comparison and not an absolute measure.

Conclusions

We have presented a novel marine seismic acquisition and processing method that utilizes continuous source and receiver side wavefields. An iterative scheme for deconvolving the source wavefield(s) extracts the response of the earth associated with each source. Multiple sources can be operated simultaneously since strong encoding minimizes the correlation between individual wavefields which facilitates an effective separation in the deconvolution step. The typical six air-gun strings towed by a seismic vessel can be configured in a way that a hexa-source setup is achieved. That potentially gives a high degree of flexibility in survey design allowing for very efficient acquisition configurations which do not sacrifice spatial sampling. When individual air-guns are triggered with dense, randomized time intervals, source energy is spread out in time which leads to reduced sound pressure levels when compared to standard air-gun arrays. This is an important step towards reducing the impact of seismic acquisition on marine life.

Acknowledgments

We thank PGS for permission to publish this paper, and Statoil and The Research Council of Norway for funding the project together with PGS.

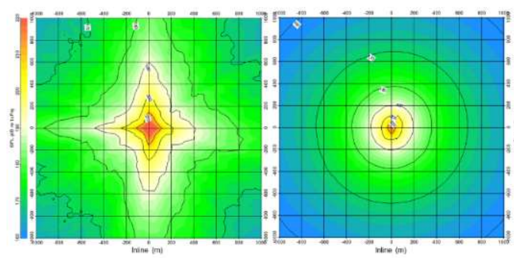

Figure 7: Peak sound pressure levels (in dB re 1 µPa) as a function of inline and cross-line distances in meters from the geometrical center of the source at a depth of 10 m (4 m below the source depth) for a conventional 4130 cubic-inch array (left) and when triggering individual air-guns in a near-continuous fashion (right).

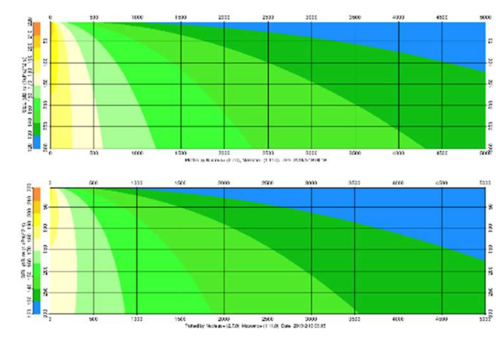

Figure 8: Sound exposure levels (in dB re 1 µPa2s) as a function of distance from the source. Horizontal axis is meters from the geometrical center of the array directly aft from the vessel, while the vertical axis is depth from the sea surface in meters. The integration time is set to 10 seconds starting from the first arrival at each location. Conventional 4130 cubic-inch array (top) is compared with triggering individual air-guns in a near-continuous fashion on the bottom.

REFERENCES

Abma, R., and A. Ross, 2013, Popcorn shooting: Sparse inversion and the distribution of airgun array energy over time: 83rd Annual International Meeting, SEG, Expanded Abstracts, 31–35, https://doi.org/10.1190/segam2013-0592.1.

Beasley, C. J., R. E. Chambers, and Z. Jiang, 1998, A new look at simultaneous sources: 68th Annual International Meeting, SEG, Expanded Abstracts, 133–135, https://doi.org/10.3997/2214-4609.201408226.

Berkhout, A. J., 2008, Changing the mindset in seismic data acquisition: The Leading Edge, **27**, 924–938, https://doi.org/10.1190/1.2954035.

Carlson, D., A. Long, W. Söllner, H. Tabti, R. Tenghamn, and N. Lunde, 2007, Increased resolution and penetration from a towed dual sensor streamer: First Break, **25**, 71–77.

Frømyr, E., G. Cambois, R. Loyd, and J. Kinkead, 2008, Flam — A simultaneous source wide azimuth test: 78th Annual International Meeting, SEG, Expanded Abstracts, 2821–2824, https://doi.org/10.1190/1.3063931.

Goertz, A., J. F. Wisløff, F. Drossaert, and J. Ali, 2013, Environmental source modelling to mitigate impact on marine life: First Break, **31**, 59–64.

Mueller, M. B., J. O. A. Robertsson, and D. F. Halliday, 2014, Simultaneous source separation using encoded source sequences: 76th Conference and Exhibition, EAGE, Extended Abstracts, Th ELI2 03, https://doi.org/10.3997/2214-4609.20141457.

Robertsson, J. O. A., L. Amundsen, and Å. Sjøen Pedersen, 2016, Wavefield signal apparition — Part I: Theory: 78th Annual International Conference and Exhibition, EAGE, Extended Abstracts, We LHR2 05, https://doi.org/10.3997/2214-4609.201600950.

Sjøen Pedersen, Å., L. Amundsen, and J. O. A. Robertsson, 2016, Wavefield Signal Apparition — Part II: Application to simultaneous sources and their separation: 78th Annual International Conference and Exhibition, EAGE, Extended Abstracts, We LHR2 06, https://doi.org/10.3997/2214-4609.201600951.

10.1190/segam2018-2995322.1